Contents lists available at SciOpen

Food Science and Human Wellness

journal homepage: https://www.sciopen.com/journal/2097-0765

China Food Publishing Co.

Effect of gallic acid on peanut protein sensitization after high moisture extrusion

Zhigang Xiao[a,b], Jiafeng Shi[a], Yanran Li[a], Keyang Sun[a], Xiaoshuai Yu[b], Yuan Yuan[a], Yuzhe Gao[a,*]

[a] College of Grain Science and Technology, Shenyang Normal University, Shenyang 110034, China
[b] College of Food, Shenyang Agricultural University, Shenyang 110866, China

ARTICLE INFO

Article history:
Received 16 December 2023
Received in revised form 6 January 2024
Accepted 4 February 2024

Keywords:
Peanut protein sensitization
High moisture extrusion
Gallic acid
Animal model

ABSTRACT

How to reduce peanut allergies has always been a main food safety concern. Plant polyphenol complex peanut sensitizing protein was proposed as a new desensitization strategy. Gallic acid (GA), as a natural plant polyphenol, has anti-inflammatory and immunomodulatory effects. Therefore, the aim of this study was to investigate the effect of GA on peanut protein (PP) sensitization under high moisture extrusion conditions. The contents of free sulfhydryl groups and disulfide bonds in the PP-GA complex were determined, and the structure of the complex was characterized by sodium dodecyl sulfate-polyacrylamide gel electrophoresis (SDS-PAGE) and Fourier transform infrared spectroscopy. The results showed that with increasing GA content, the number of free sulfhydryl groups increased while the number of disulfide bonds decreased. The secondary structure of PP-GA showed that the random coils and β-turns were transformed to α-helices and β-sheets. A BALB/c mouse model was also established, wherein $Al(OH)_3$ was used as an adjuvant when the complex was administered via intraperitoneal injection, and the mice showed mild allergic symptoms and a decreased immune organ index. In addition, the serum levels of specific antibodies (immunoglobulin E (IgE), immunoglobulin G1 (IgG1), and immunoglobulin G2a (IgG2a)), cytokines (interleukin-5 (IL-5), interleukin-13 (IL-13), and interferon gamma (IFN-γ)) and histamine were reduced. In summary, this study proved that GA can relieve the sensitization of PP induced by high moisture extrusion.

1. Introduction

Food allergies have always been a key concern worldwide. The Food and Agriculture Organization of the United Nations (FAO) has identified milk, eggs, nuts, soybeans, peanuts, wheat, fish and shellfish as the top 8 allergens[1-2]. However, allergic reactions to peanuts are of greater concern, and peanut allergy patients will show gastrointestinal discomfort, erythema papules, urticaria, a drop in blood pressure, angioedema and other symptoms. If the situation is serious, anaphylactic shock may result, or the reaction could even be life-threatening[3-4]. More than 50% of food allergy-related deaths are caused by peanuts, and more than 40% of children with food allergies are allergic to peanuts[5]. However, peanut products are widely used in the daily diet, and there have been peanut allergy patients that directly or indirectly ingest the peanut allergen due to accidental factors.

High water extrusion is a new representative modification technology. Under high temperature, high pressure and high shear force conditions, the original chemical bonds within or between peanut proteins (PP) are destroyed, the molecular chains become extended, the hydrophobic and sulfhydryl groups buried inside the

* Corresponding authors at: College of Grain Science and Technology, Shenyang Normal University, Shenyang 110034, China
E-mail address: gyz157024@126.com (Y.Z. Gao)
Peer review under responsibility of Beijing Academy of Food Sciences.

SciOpen Publishing services by Tsinghua University Press

http://doi.org/10.26599/FSHW.2024.9250196

protein are exposed, and association, aggregation, crosslinking, decomposition, oxidation, reduction and other reactions can occur within and between molecules[6]. PP molecules rearrange and polymerize to form a new ordered network structure, resulting in changes in the structures of peanut-sensitizing proteins, which can reduce PP sensitization. Although these treatments (heat, high pressure, ultrasound, radiation or enzymatic hydrolysis, etc.) can reduce PP sensitization to a certain extent, they have certain limitations in terms of their safety and application scope and will also lead to a loss in the nutritional value of the food itself[7-8].

As a plant polyphenol, gallic acid (GA) is a natural active substance that is green and safe, with antiaging, antioxidative and antibacterial effects[9]. In addition, polyphenols such as GA have a strong binding affinity for proteins. Studies have shown that plant polyphenols can reduce PP sensitization in two ways: (1) plant polyphenols interfere with PP allergic reactions, and (2) plant polyphenols and PP complexes indirectly regulate allergic reactions. Therefore, plant polyphenols complexed with sensitizing proteins have been proposed as a new desensitization strategy[10]. He et al.[11] covalently bound epigallocatechin gallate (EGCG) and chlorogenic acid (CHA) to the peanut-sensitizing protein Arah1. The experimental data showed that the specific immunoglobulin E (IgE) antibody binding ability of the peanut-sensitizing protein Arah1 was reduced, and histamine (HIS) release from basophils (KU812 cells) was significantly lowered. Plundrich et al.[12] combined proanthocyanidin C1 and CHA with Arah2, which resulted in significant 37% and 50% reductions in IgE binding capacity.

In this study, PP was cotreated via high moisture extrusion and with GA, and the effect of GA content on PP sensitization was evaluated in a mouse model. The data here provide basic research results and technical support for reducing PP sensitization in the future.

2. Materials and methods

2.1 Materials

PP was purchased from Shandong Yuwang Industrial Co., Ltd. (Shandong, China). GA was purchased from Shanghai McLean Biochemical Technology Co., Ltd. (Shanghai, China) with a purity of 99.00%. Four- to six-week-old female BALB/c mice were supplied by Shenyang Yuwang Biotechnology Co., Ltd. (Liaoning, China). The enzyme-linked immunosorbent assay (ELISA) kit was purchased from Jiangsu Jingmei Biotechnology Co., Ltd. (Yancheng, China). All other chemicals were of analytical grade.

2.2 Extrusion experiments

A double screw extruder was used in the extrusion experiment with 5 zones in the barrel. PP and polyphenols can interact under high temperature, high pressure and high shear force conditions. According to data from previous studies, the feeding speed was set to 6 kg/h, screw speed (SS) to 240 r/min, and moisture concentration (MC) to 50%, and the temperatures (T) in the 5 zones were 60, 90, 150, and 110 ℃ to ensure that the components of the mixture would interact in the extruder and be extruded at a constant rate. Based on the weight of PP, the concentration of GA (GAC) was set to 0%, 2%, 4%, 6% and 8% (*m*/*m*) to investigate the effect of GAC on the PP sensitization after extrusion.

2.3 Determination of the GA binding rate

The content of GA in the PP-GA complex was determined by the Folin-phenol method[13]. One milliliter of sample solution with a concentration of 2 mg/mL was added to 2.5 mL of 0.2 mol/L Folin-phenol reagent, and then 2 mL of 7.5 g/100 mL Na_2CO_3 solution was added for 5 min of reaction in the dark. After the reaction continued in the dark for 2 h, the absorbance of the solution was measured at a wavelength of 760 nm. The standard curve of GA was drawn, and the binding rate of GA was calculated according to formula (1):

$$\text{GA binding rate}\,(\%) = \frac{\text{Determination of GA}}{\text{GA addition}} \times 100 \quad (1)$$

2.4 Determination of the contents of free sulfhydryls and disulfide bonds

A 5 mg/mL sample solution was prepared with Tris-glycine buffer containing 8 mol/L urea (0.086 mol/L Tris, 0.09 mol/L glycine and 4 mmol/L ethylene diamine tetraacetic acid, pH 8.0), magnetically stirred for 30 min, and then centrifuged for 10 min at 6 000 r/min. The supernatant was collected for determination.

Determination of free sulfhydryl group content: First, 5 mL of supernatant was added to 50 μL of Ellman's reagent (4 mg/mL), the reaction was carried out in the dark for 15 min, after which the absorbance was measured at 412 nm[14]. A sample without added protein was used as a blank control. The content of free sulfhydryl groups was calculated according to formula (2):

$$\text{Free sulfhydryl content}\,((\mu\text{mol}/(\text{L}\cdot\text{g})) = \frac{73.53 \times A_{412\,\text{nm}} \times D}{C} \quad (2)$$

Where, $A_{412\,\text{nm}}$ is the absorption value of the sample at 412 nm, D is the dilution ratio and C is the sample concentration (mg/mL).

Total sulfhydryl content (TSC) determination: First, 1 mL of supernatant was added to 10 μL of β-mercaptoethanol and 4 mL of Tris-glycine buffer, and the mixture was held at room temperature for 1 h. Then, 10 mL of 12% trichloroacetic acid was added, and the mixture was shaken to homogeneity, allowed to fully react for 1 h, and centrifuged at 6 000 r/min for 10 min, after which the precipitate was collected. Next, 10 mL of Tris-glycine buffer was added, and the mixture was oscillated to fully dissolve the precipitate. 4 mL of the solution was added to 40 μL of Ellman's reagent, and the reaction was carried out in the dark for 15 min. The absorbance of the solution was then measured at 412 nm, and a sample without added protein was used as a blank control[15]. The disulfide bond content was calculated according to formula (3):

$$\text{Disulfide bond content}\,(\mu\text{mol}/(\text{L}\cdot\text{g})) = \frac{\text{TSC} - \text{Free sulfhydryl content}}{2} \quad (3)$$

2.5 Sodium dodecyl sulfate-polyacrylamide gel electrophoresis (SDS-PAGE)

The molecular weight distributions of PP and its complex with GA were analyzed by SDS-PAGE[16]. First, a sample (2 mg) was dissolved in 0.5 mL of sample buffer (0.08 mol/L Tris-HCl buffer, pH 6.8), 1% SDS, 2% (*V*/*V*) 2-β-mercaptoethanol, 5% (*V*/*V*) glycerol, and 0.025% bromophenol blue and mixed well. Each sample was

heated in a boiling water bath for 10 min and centrifuged at 6 000 × *g* for 10 min. The supernatant (4 μL) was placed in a stacked gel tank, and commercial molecular weight markers with molecular weights ranging from 5 kDa to 250 kDa were applied. Using the Mini-PROTEAN® system, electrophoresis was performed in run tank buffer (0.025 mol/L Tris, 0.192 mol/L glycine, pH 8.6−8.7) at 80 V until the trace dye entered the stacked gel and then increased to 120 V into the dissolved gel. The gel was stained for 30 min with staining solution (500 mL of methanol, 68 mL of glacial acetic acid, and 432 mL of deionized water) and 40 min with a solution of Coomassie bright blue (1 g of Coomassie bright blue (R-250), 500 mL of methanol, 68 mL of glacial acetic acid, and 432 mL of deionized water). The gel was then treated with decolorizing solution (75 mL of glacial acetic acid, 50 mL of ethanol, and 875 mL of deionized water) three times for 12 h overnight. Protein electrophoretic data were imaged using an AlphaEase FC gel imaging system.

2.6 Scanning electron microscopy (SEM)

SEM was used to observe the microscopic morphology of the samples[17]. A small number of particles were fixed on the sample table with conductive double-sided adhesive, and an ion sputtering instrument was used to spray the surface with gold at 20 mA for 45 s. The gold-treated sample was put into the sample room, observed at 15 kV and photographed.

2.7 Fourier transform infrared spectroscopy (FT-IR)

The samples were scanned by a Nicolet 5DXC infrared spectrometer[18]. Spectra were acquired in the range of 4 000−400 cm^{-1} with a resolution of 4 cm^{-1}. Moreover, Peakfit version 4.12 software was used for spectral processing, and the contents of each secondary structure component in the sample was calculated by the Peakfit software.

2.8 Animal experimental design

Forty-nine female BALB/c mice aged 4−6 weeks were randomly divided into 7 groups, with 7 mice in each group (the specifics of which follow). The experiment was conducted in strict compliance with Chinese Animal Welfare Guidelines and approved by Ethics Committee of College of Grain Science and Technology, Shenyang Normal University (date of approval 17 May 2023 and protocol number 2023-000517). The mice were housed on a 12 h/12 h light/dark cycle at a temperature of (22 ± 1) ℃ and humidity of 45%−55% with free access to food and drink. The model was established after 1 week of adaptive feeding. Modeling and treatment were carried out according to the experimental groupings. The experimental procedure is shown in Fig. 1. The specific method was as follows: 0.5 mL of normal saline (containing 100 μg of PP + 1 mg of $Al(OH)_3$ adjuvant) was intraperitoneally injected into the mice on the 7th, 14th, 21st and 28th days, except for the mice in the blank control group. On the 35th day, the model group was intraperitoneally injected with 0.5 mL of normal saline (containing 200 μg of PP). The GA group was intraperitoneally injected with 0.5 mL of PP-GA complex containing different doses of gallate GA (2%, 4%, 6%, or 8% with 200 μg of PP in the complex). The blank control group was given an equal volume of normal saline throughout this whole process. Thirty minutes after intraperitoneal injection of the samples, the eyeballs of the mice were removed, blood was taken from the mice, and the spleen, peritoneal lavage fluid, jejunum and lung tissues were removed. The blood was stored at 4 ℃ overnight and centrifuged at 4 ℃ and 5 000 r/min for 10 min, and the upper serum (approximately 100 μL) was separated and stored at −20 ℃[19].

2.9 Mouse allergy symptom score

The symptoms of mice in each group were observed 30 min after each intragastric treatment, and allergy symptoms were scored according to Table 1[20].

2.10 Mouse rate of body weight gain and splenic mass fraction

The body weights of the mice in each group were recorded before intragastric administration on days 0, 7, 14, 21 and 28. The spleens of the mice were also weighed, and the rate of weight gain and splenic mass fraction were calculated by formula (4) and formula (5):

$$\text{Weight gain rate}\,(\%) = \frac{m_n - m_0}{m_0} \times 100 \quad (4)$$

$$\text{Splenic growth rate}\,(\%) = \frac{m_{S35}}{m_{35}} \times 100 \quad (5)$$

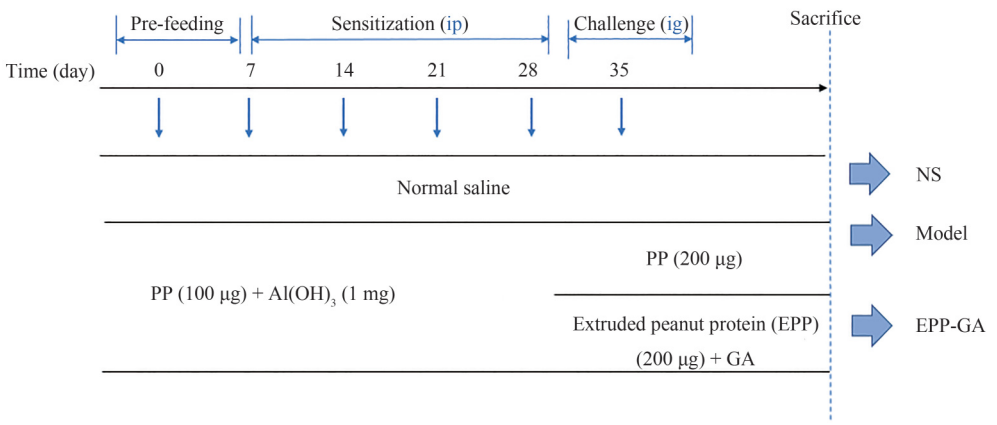

Fig. 1 Establishment of the PP allergy BALB/c mouse model.

Where, m_0, m_{35} and m_n are the body weights of mice on day 0, day 35 and day n, respectively, and m_{S35} is the masses of the spleen on day 35, respectively.

Table 1
Anaphylactic symptom scoring of allergic mice.

Score	Symptoms
0	Absence of symptoms
1	Scratching the nose and head, hair rising
2	Puffiness around the eyes and mouth, pilar erecti, diarrhea and reduced activity or tachypnea
3	Wheezing, dorsiflexion and dyspnea
4	Loss of consciousness and tremors
5	Shock and death

2.11 Observation of mast cells and basophil granulocytes in mouse peritoneal lavage fluid

During dissection of the BALB/c mice, 3 mL of Hank's solution was injected into the abdominal cavity, gentle massaging was performed for 1 min, and then the solution was removed. The diluted cell solution (200−500 μL) was added to a slide and left to dry. After staining with toluidine blue solution for 2 min, the surface of the slide was rinsed with water until the staining solution had been removed, and then the slide was left to dry. The morphologies of the mast cells and basophils in the peritoneal lavage solution were observed under an optical microscope[21].

2.12 Hematoxylin and eosin (H&E) staining

The jejunum and lung tissues of BALB/c mice were cut into pieces with appropriate volumes, soaked in 4% paraformaldehyde for preservation, made transparent by treatment with xylene, embedded in paraffin, sliced into 5 μm slices with a microtome, and stained with H&E. Pathological changes in the mouse jejunum and lung were observed under an optical microscope. Peribronchiolar inflammatory cell infiltration, alveolar inflammatory cell infiltration, alveolar wall thickening, alveolar stenosis and macrophage infiltration were used to evaluate the degree of inflammation[22].

2.13 Assays for specific IgE, IgG1 and IgG2a antibodies

The contents of PP-specific immunoglobulin E (IgE), immunoglobulin G1 (IgG1), and immunoglobulin G2a (IgG2a) in mouse samples were determined by a double antigen sandwich assay using a commercial ELISA kit. A blank well (blank control well without the addition of sample or enzyme-labeled reagent; the other steps were the same), a standard well, and a sample well were used for analysis. Fifty microliters of standard material was accurately added to the enzyme label-coated plate, 40 μL of sample diluent was added to the sample well to be tested, and then 10 μL of sample to be tested was added at a final sample dilution of 5-fold. The sample was added to the bottom of the well, taking care to not touch the wall, and the plate was gently shaken and mixed. After sealing the plate with film, the plate was incubated at 37 ℃ for 30 min. Next, concentrated washing liquid was diluted 30-fold with distilled water for reserve use, the film was carefully removed from the plate, and the liquid was discarded and the plate was shaken to dry. Then, each well was filled with washing liquid and left to stand for 30 s before discarding the liquid; this step was repeated 5 times. After patting dry, 50 μL of enzyme-labeled reagent was added to each well (except the blank wells), the plate was incubated in a warm bath and washed again, and color developing agent A (50 μL) was added to each well. Then, color developing agent B (50 μL) was added and the plate was gently shaken and mixed and incubated in the dark for 10 min at 37 ℃. After adding termination solution (50 μL/well) to terminate the reaction (at this time, the blue wells immediately turned yellow), the blank well was adjusted according to the standard, and the optical density (OD) value of each well was measured at 450 nm. The contents of peanut-specific IgE, IgG1 and IgG2a antibodies were determined according to the standard curve. Cytokine and plasma HIS levels were also assessed.

2.14 Determination of IL-5, IL-13, IFN-γ and HIS in mouse serum

The contents of interleukin-5 (IL-5), interleukin-13 (IL-13), interferon gamma (IFN-γ) and HIS in serum were determined by a double antibody sandwich ELISA kit. The specific experimental steps are given in Section 2.13. The OD values of the prepared solutions from the BALB/c mice were measured by the enzyme labeling method at a wavelength of 450 nm. The levels of IL-5, IL-13, IFN-γ and HIS in the serum of mice were determined by the standard curve method.

2.15 Statistical analysis

The mentioned tests were performed in at least triplicate. All data are expressed as the mean ± SD. Data were analyzed by one-way ANOVA and Duncan's test by using SPSS software. $P < 0.05$ was considered to indicate a significant difference.

3. Results and discussion

3.1 Analysis of binding rates

According to the results in Fig. 2, with the addition of GA in the range of 2%−8%, the amount of PP bound increased from 17.35 μg to 77.38 μg. This was because the carbonyl or amide groups in the amino acid sequence of the PP bind to the hydroxyl groups of GA[23]. However, when 6% GA was present, the PP-GA combination rate was the highest, reaching 50.30%. When there was 8% GA, the binding rate decreased, which may be due to two reasons: 1) After PP binds to GA, the structure of the protein changes, and some GA and PP binding sites are buried; 2) After the binding of GA and PP approaches saturation, the addition of more GA will make the denominator in the calculation formula (the added amount of GA) continue to increase, resulting in a decrease in the overall calculated value; this is consistent with the report of Jin et al.[24].

3.2 Analysis of the contents of free sulfhydryl groups and disulfide bonds

Disulfide bonds play important roles in the secondary and tertiary structures of proteins[25]. Sulfhydryl groups exist as free groups or disulfide bonds, and changes to the free sulfhydryl groups cause

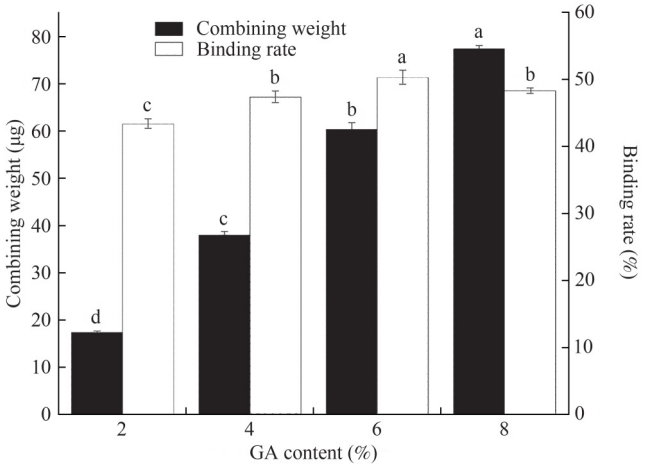

Fig. 2 Amount and rate of GA and PP binding under high moisture extrusion conditions. Different lowercase letters in same index indicate significant differences among all groups ($P < 0.05$). The same as below.

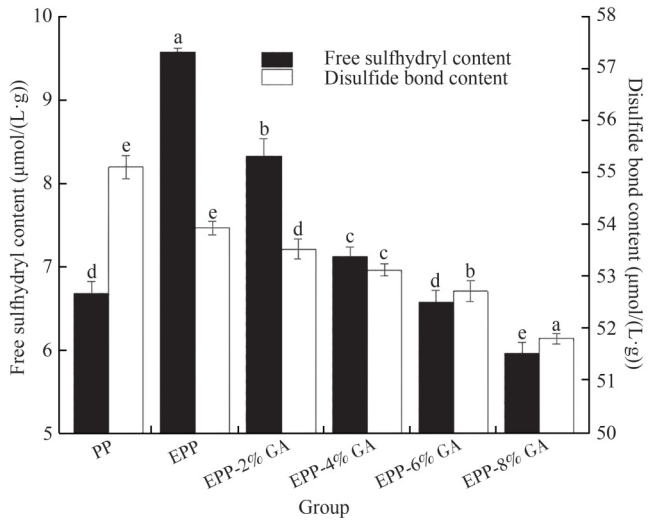

Fig. 3 Effect of GA on the contents of free sulfhydryl groups and disulfide bonds in PP after high moisture extrusion.

structural changes in proteins. Free sulfhydryl groups and disulfide bonds are important components that maintain the structural stability of the PP-GA complex[26]. As shown in Fig. 3, the content of free sulfhydryl groups in PP increased from 6.69 μmol/(L·g) to 9.58 μmol/(L·g) and the content of disulfide bonds decreased from 8.35 μmol/(L·g) to 6.75 μmol/(L·g) after extrusion. After high moisture extrusion processing, the intermolecular disulfide bonds were broken due to the mechanical shear and high temperature conditions, exposing more sulfhydryl groups[27]. The results showed sulfhydryl group-disulfide bond exchange after high moisture extrusion of PP. With increasing GA supplementation, the content of free sulfhydryl groups in the complex significantly increased, while the content of disulfide bonds significantly decreased ($P < 0.05$). When the content of GA was 8%, the content of free sulfhydryl groups increased to 5.96 μmol/(L·g), and the content of disulfide bonds decreased to 51.83 μmol/(L·g). Urea was added to determine the content of free sulfhydryl groups in the PP-GA complex, as this method can exclude changes in the free sulfhydryl group content caused by the transformation of disulfide bonds[28]. Therefore, the reduction in the content of free sulfhydryl groups is the result of the sulfhydryl groups in PP combining with the phenolic hydroxyl groups in GA[29]. Meng et al.[30] also reached the same conclusion: whey protein isolate formed noncovalent interactions with polyphenols, which significantly reduced the content of sulfhydryl groups. The decrease in disulfide bond content is mainly due to the introduction of phenolic hydroxyl groups in the PP structure, and the steric effects of the GA aromatic ring causes the disulfide bonds in PP to break. In addition, the lowered disulfide bond content is also due to the antioxidant effects of GA, which inhibits the oxidation of sulfhydryl groups to quinones and prevents the formation of more new disulfide bonds[31]. Many studies have shown that the amount of added polyphenol is positively correlated with its antioxidant capacity. Therefore, when more GA is added, the antioxidant capacity becomes stronger and the lower the disulfide bond content in the PP-GA complex is.

3.3 SDS-PAGE analysis

SDS-PAGE can indicate the molecular weight distribution of the subunits in PP and its complexes with GA. Arah1, Arah2 and Arah3 were the main peanut sensitizing proteins, and their molecular weights were 64, 16−18, and 61 kDa, respectively. These proteins accounted for 12%–16%, 5.9%–9.3%, and 3.7%–4.3% of the total PP, respectively, and could be recognized by 90% of the serum samples from allergic patients[32-33]. As shown in Fig. 4, after high moisture extrusion, the PP bands with molecular weights of 18, 37 and 65 kDa became obviously lighter. These changes were attributed to the fact that under high moisture extrusion conditions, PP was subjected to high temperature, high pressure and mechanical shear forces, which cleaved peptide bonds and decomposed the protein into subunits with relatively small molecular weights. With the increase in the amount of GA, the bands of the PP-GA complexes at approximately 18, 37 and 65 kDa became lighter to varying degrees. When the amount of GA was 8%, the band at approximately 65 kDa disappeared. These results showed that an interaction between PP and GA occurred under high moisture extrusion conditions, and the content of sensitizing protein subunits decreased. According to the SDS-PAGE results, sensitization to PP-GA is lower than that to untreated PP, and sensitization to the complex is lowest when the amount of GA is 8% under high water extrusion conditions.

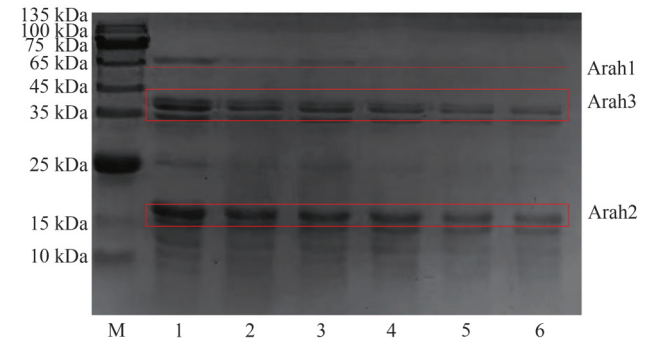

Fig. 4 SDS-PAGE of PP and the PP-GA complexes under high moisture extrusion conditions. M. Standard molecular weight protein marker, 1. PP, 2. EPP, 3. EPP-2% GA, 4. EPP-4% GA, 5. EPP-6% GA, and 6. EPP-8% GA.

3.4 Analysis of microstructural changes in the PP-GA complexes

According to Fig. 5, the PP particle sizes were different after complexation, their surfaces were rough, and the particle gap was

small at 400× magnification. After extrusion, the number of small particles was significantly reduced, and the particle size tended to be average. Under the combined actions of high temperature, high pressure and mechanical shear force of the twin screw extruder, the PP structure stretched, hydrogen bonds were broken, hydrophobic groups decomposed into smaller particles, and the particles reunited at the reducing end, thus forming particles of relatively average size[34]. The 5 000× magnification images showed that after the addition of GA, the morphology of the PP complex changed significantly, the particle size decreased, the surface was smooth, and the distribution was relatively dispersed, which may be because the binding of GA with PP weakened the forces of aggregation between the PPs. The particle size of the PP-GA complex formed under extrusion tended to be average, and the surface was smooth. Other experiments came to this same conclusion, as GA changed the microstructure of casein due to hydrophobic interactions, resulting in casein having a loosely distributed structure[35].

3.5 Analysis of the changes in the secondary structure of PP-GA complex

FT-IR mainly relies on the stretching vibrations between atoms inside a molecule to effectively detect the changes in protein functional groups and can effectively identify the functional groups contained in proteins. Proteins have 4 major amide bands as follows: the amide A band appears at 3 100−3 700 cm^{-1}, amide B at 2 800−3 000 cm^{-1}, amide I at 1 600−1 700 cm^{-1}, and amide II at 1 500−1 600 cm^{-1}. Fig. 6 shows that the infrared spectra of PP and its complexes with GA have a strong absorption peak in the range of the amide A band, which is related to intermolecular hydrogen bonding and the stretching vibrations of O−H and N−H[36]. The changes in the positions of the amide A and amide B bands indicate that GA mainly forms hydrogen bonds and hydrophobic interactions with PP[37]. The changes in the amide I and amide II bands were due to interactions between the oxygen atoms and the hydroxyl groups on GA with the C−O and C−N groups on the protein, resulting in a rearrangement of the PP chain and changes in its secondary structure, which is related to C=O stretching, N−H bending and C−N stretching vibrations[38]. In the amide I region, the absorption peak of PP-GA decreased significantly with increasing amounts of GA, indicating that the interaction between PP and GA exposed more nonpolar groups, such as hydrophobic groups, and changed the structure of PP under the conditions of high moisture extrusion.

To further study the effect of GA addition on the conformational changes in PP and determine if the secondary structure of the protein in the amide I region was sensitive to change[39], Fourier deconvolution and second derivative fitting of the absorption peak within its range were conducted, the secondary structure composition was analyzed, and the content of each secondary structure feature was calculated according to the peak area for each sample. Generally, secondary structures have bands in certain ranges as follows: β-sheets (1 600−1 640 cm^{-1}), random coils (1 640−1 650 cm^{-1}), α-helices

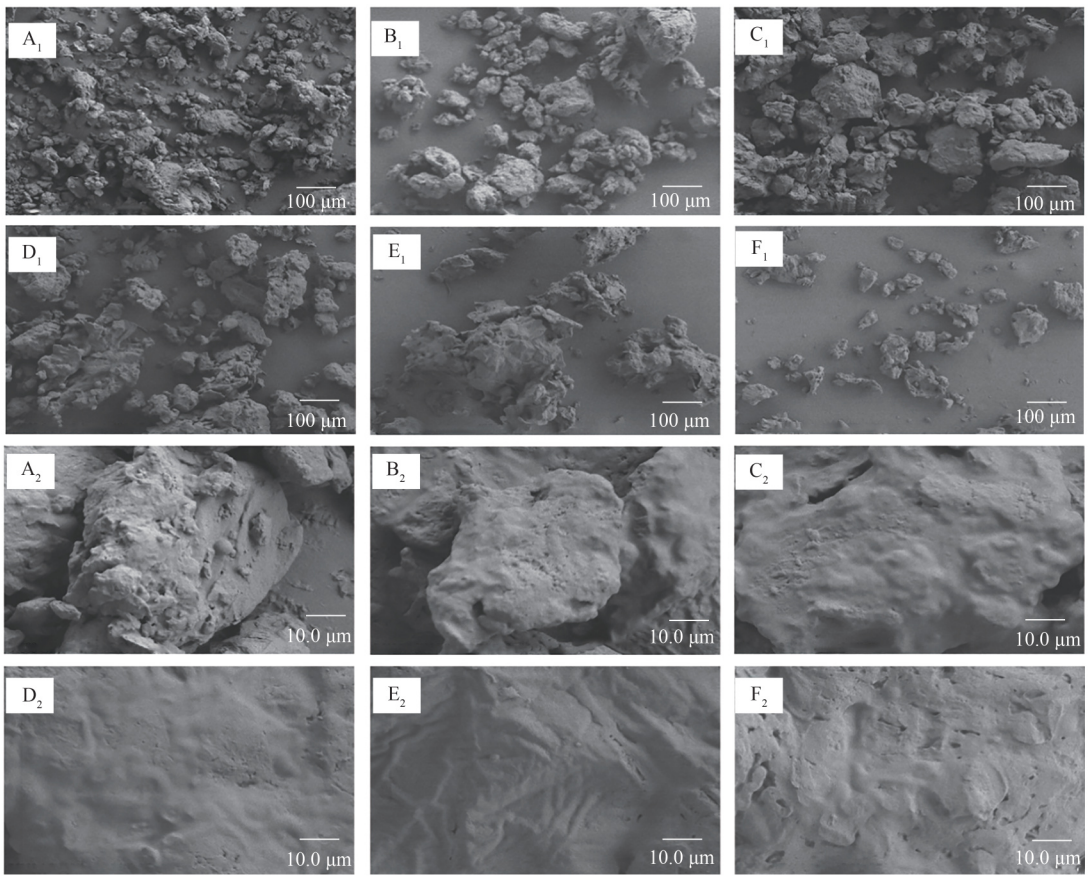

Fig. 5 Microstructures of PP and PP-GA obtained by SEM in the process of high moisture extrusion. (A_1-F_1) The microstructures of the PP and PP-GA complex samples were observed by SEM at 400× magnification. (A_2-F_2) The microstructures of the PP and PP-GA complex samples were observed by SEM at 5 000× magnification. (A) PP, (B) EPP, (C) EPP-2% GA, (D) EPP-4% GA, (E) EPP-6% GA, and (F) EPP-8% GA.

(1 650−1 660 cm^{-1}), and β-turns (1 660−1 700 cm^{-1}) [40-41]. The stability of the β-sheet structure was determined by hydrogen bonds between polypeptide chains, α-helices are usually formed by intramolecular hydrogen bonds between amino hydrogen (NH−) and carbonyl oxygen (−CO) groups, β-turns form via weak hydrogen bonding structures, and random coils are generated in the unfolded configuration and are related to the flexibility of the protein[42].

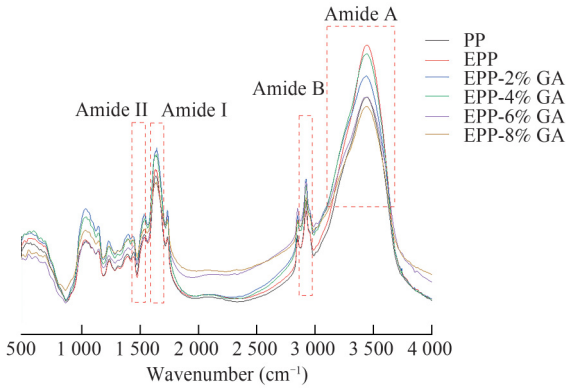

Fig. 6 FT-IR of PP and the PP-GA complexes under high moisture extrusion conditions in the range of 500−4 000 cm^{-1}.

As shown in Table 2, the main secondary structure of PP is the β-sheet with a content of 32.36%, and the contents of random coils, α-helices and β-turns were 22.04%, 21.22% and 24.71%, respectively. After high moisture extrusion, the contents of α-helices and β-sheets in the PP secondary structure decreased by 4.07% and 3.87%, respectively, while the contents of random coils and β-turns increased by 4.38% and 1.56%, respectively. Hydrogen bonding was the main force that maintained the α-helices structure. Under the conditions of high moisture extrusion, PP was subjected to high temperature, high pressure and mechanical shear, breaking the internal hydrogen bonds and resulting in a reduction in the α-helices content. α-Helices and β-sheets are related to the ordered structure of the protein. The transformation of β-sheets and α-helices to random coils and β-turns indicated that the structure of PP tended to be disordered due to high water compression[43]. After the addition of GA and its increase in concentration, the contents of random coils and β-turns decreased gradually, while the contents of α-helices and β-sheets increased gradually. This was attributed to the fact that the chemical groups of GA can participate in hydrogen bonding and hydrophobic interactions with PP residues, changing the contents of each type of secondary structure with a tendency to make the molecular structure of PP-GA ordered. However, when the amount of GA was 8%, the β-sheet content decreased because under the actions of GA, the β-sheets in the PP structure were transformed into more stable α-helices. Zhao et al.[44] also reached the same conclusion: EGCG had a regulatory effect on protein secondary structure. Therefore, GA could interact with PP under the conditions of high moisture extrusion, thus changing the structure of PP and inducing it to be more ordered.

3.6 *Analysis of the mouse allergy symptom scores*

Food allergy symptoms are the result of a comprehensive immune response that includes the systemic, gastrointestinal, and mucosal immune systems. The allergy symptom score is the most direct method by which allergies in mice can be reflected and can be used as an important index to evaluate the occurrence and severity of food allergies[45]. The symptoms of the mice in each group were scored 30 min after intraperitoneal injection of the appropriate sample on day 35 according to the reference table. According to Fig. 7, the NS group of mice showed normal performance, good activity, and no allergic reaction symptoms. Mice in the Model group and GA group showed different degrees of allergic symptoms after the final sensitization stimulation. To a certain extent, these results indicate that intraperitoneal injection of PP solution with $Al(OH)_3$ as an adjuvant can successfully establish a BALB/c mouse model of peanut allergy[46]. As shown in Fig. 7, there was no significant difference in allergic symptoms between the Model group and the 0% GA group ($P > 0.05$). Specifically, four mice in each the Model group and 0% GA group showed dyspnea and cyanosis of the mouth and tail, three mice showed edema around the eyes, diarrhea, pilar erecti, reduced activity and an increased respiratory rate. With the increase in GA supplementation, the allergic symptom scores of the mice decreased, and the extent of the allergic reaction was reduced. Compared with the Model group (2.57), the average allergy symptom score of the mice in the 8% GA group was reduced to 1.71, showing only grade 1 to 2 allergy symptoms. The allergy symptom score results showed that the extent of the allergic reaction caused by PP combined with GA was reduced.

Table 2
Proportions (%) of each secondary structure in PP and the PP-GA complexes under high water extrusion conditions.

Group	β-Sheet	Random coil	α-Helix	β-Turn
PP	32.36 ± 0.18^{a}	22.04 ± 0.73^{e}	21.22 ± 0.39^{c}	24.71 ± 0.29^{b}
EPP	28.49 ± 0.40^{d}	26.42 ± 0.09^{a}	17.15 ± 0.74^{e}	26.27 ± 0.16^{a}
EPP-2% GA	29.53 ± 0.26^{c}	25.51 ± 0.42^{b}	19.51 ± 0.34^{d}	24.45 ± 0.40^{b}
EPP-4% GA	29.71 ± 0.27^{c}	24.54 ± 0.38^{c}	21.58 ± 0.36^{c}	23.29 ± 0.17^{c}
EPP-6% GA	30.51 ± 0.30^{b}	24.42 ± 0.04^{c}	23.50 ± 0.31^{b}	22.46 ± 0.38^{d}
EPP-8% GA	29.65 ± 0.39^{c}	23.35 ± 0.31^{d}	25.66 ± 0.26^{a}	21.34 ± 0.38^{e}

Note: Different lowercase letters in same index indicate significant differences among all groups ($P < 0.05$).

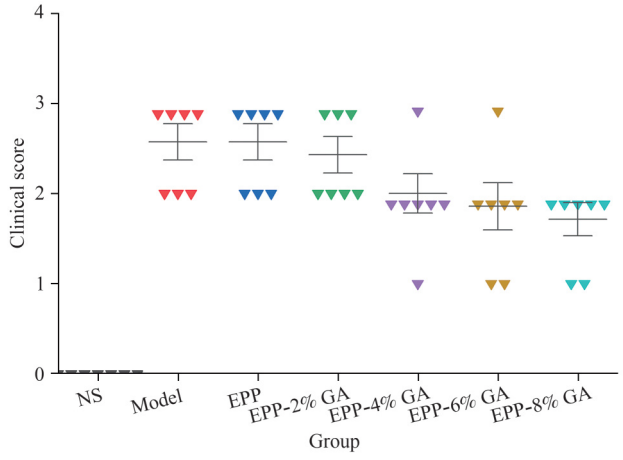

Fig. 7 Clinical allergy symptom scores of mice in each group ($n = 7$).

3.7 Analysis of the mouse rate of body weight gain and splenic mass fraction

Peanut allergy affects the body's digestive functions and a reaction could result the adverse effects of diarrhea, vomiting, and constipation, thus affecting weight[47]. The body weights of the mice in each group were observed and recorded throughout the sensitization period. As shown in Fig. 8, the weights of the mice in each group increased steadily. The rates of body weight gain of the mice in the NS group were 17.77%, 18.40%, 18.81%, 19.21% and 19.71% at days 7, 14, 21, 28 and 35, respectively, showing the highest overall growth rate, while the rates of body weight gain of the mice in the Model group were lower than those of the mice in the NS group during the same period. These rates in the Model group were 17.66%, 18.03%, 18.36%, 18.69% and 19.00%, respectively, indicating that these mice suffered from inflammation, decreased appetite or anxiety due to peanut allergy, which reduced the body weight gain. The rate of body weight gain in the GA group was between those in the NS group and Model group. There was no significant difference in body weight growth rate between GA groups ($P > 0.05$). It could thus be inferred that mice that had received intraperitoneal injection of PP-GA had a mild allergy, which had little influence on appetite and digestive ability, resulting in a smaller change in weight[48].

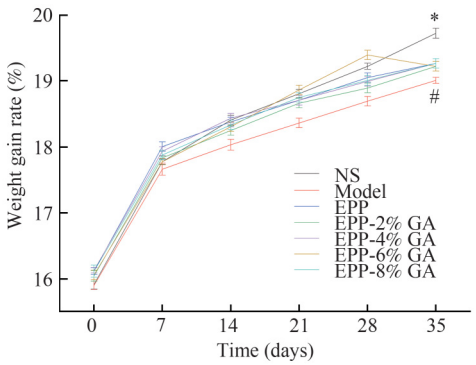

Fig. 8 Weight gain of the mice in each group during the immunization period (days 0−35). Significant differences between NS group and other groups, $^{*}P < 0.05$; Significant differences between Model group and other groups, $^{\#}P < 0.05$.

As an important immune organ, the spleen plays a major regulatory role in the immune response. When an antigen is present, macrophages and lymphocytes in the spleen mount an immune response and engulf the antigen, causing the spleen to swell. Therefore, the spleen index can be used as an index to evaluate the degree of sensitization[49]. As shown in Fig. 9, compared with the NS group (0.54%), the spleen index of the Model group mice was the largest (0.68%), and this increase in the spleen index indicated that the spleen produced an immune response to the antigen and that the immune function in the animal was enhanced[50]. However, with the increase in GA supplementation, the spleen indices of the mice decreased gradually but remained higher than that in the NS group. Within a certain range, with increasing GA content, the inhibitory effect was more obvious. When the GA content was 8%, the spleen index of the mice was 0.58%. These results showed that peanut allergy could lead to splenomegaly in mice, while the presence of GA could inhibit splenomegaly. Therefore, it could be inferred that the combination of PP and GA can alleviate spleen enlargement in mice.

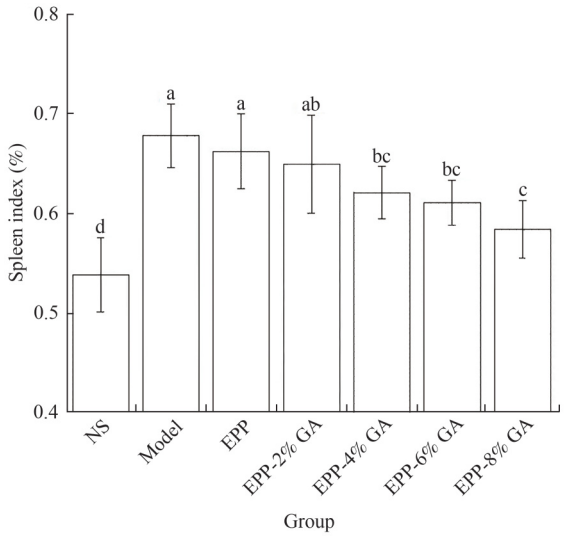

Fig. 9 Spleen index in mice in each group after the 35-day experimental period ($n = 7$).

3.8 Analysis of mast cells and basophils

During an immune reaction, mast cells in the mucosa or connective tissue will degranulate under the stimulation of the allergen, releasing HIS, heparin, interleukin and other bioactive mediators[51]. Basophilic particles can be stained with toluidine blue to appear purple. As shown in Fig. 10, degranulation was not observed in the NS group, but the Model group and GA group showed degranulation to varying degrees. The degranulation of mast cells and basophilic granulocytes was the highest and most obvious in the Model group, indicating that untreated PP may produce higher sensitization. With the addition of different amounts of GA, the degree of aggregation of mast cells and basophils was significantly reduced, and the proportion of aggregation was smaller with 8% GA. These results indicated that GA could effectively inhibit the degranulation of mast cells and basophils, and this effect was the best when the amount of GA was 8%. The extent of degranulation caused by the PP-GA complex is relatively small, so it could be inferred that sensitization to the PP and GA complex formed under high moisture extrusion conditions was lower than that to untreated PP that combining PP with GA is an effective way to reduce sensitization to PP.

3.9 Physical analysis of intestinal and lung disease

Food allergies are related to defects in intestinal barrier function, and when antigens cross the dysfunctional intestinal barrier, this leads to mast cell recruitment, the production of specific IgE antibodies, the secretion of T helper 2 cell (Th2)-related cytokines, and finally the allergic reaction in the body[52]. Therefore, observations of the intestinal morphology could be used to indicate and evaluate intestinal structure and function.

As shown in Figs. $11A_1$-G_1, the intestinal villi of mice in the NS group were slender and tightly arranged, the intestinal mucosa structure was complete, the lamina propria was abundant in columnar

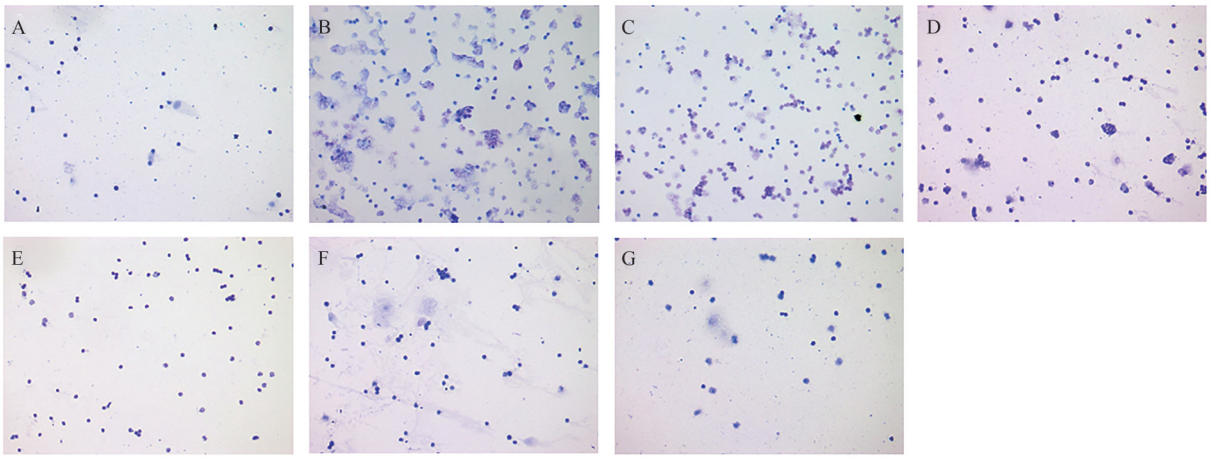

Fig. 10 Morphologies of mast cells and basophilic granulocytes in peritoneal lavage were observed under an optical microscope. (A) NS, (B) PP, (C) EPP, (D) EPP-2% GA, (E) EPP-4% GA, (F) EPP-6% GA, and (G) EPP-8% GA.

and goblet cells, and no obvious inflammation was observed. In the Model group, the intestinal villi were severely ruptured, blood cells had infiltrated, the villi were atrophied and broken, and the number of endothelial cells decreased. The intestinal wall of mice in the 0% GA group was thickened and inflammation was more obvious, indicating continued sensitization to PP after high water extrusion treatment; however, the immune response caused by the allergy was reduced. Moreover, the intestinal villi in the GA-supplemented mice were broken to varying degrees, but the extent of damage to the jejunum structure was reduced. Morphological analysis showed that PP-GA could repair the structure and function of the intestinal barrier and improve peanut allergy in mice.

As shown in Figs. 11A_2-G_2, the lung tissue structure in the mice in the NS group was clear, and the bronchus was intact. Endobronchial epithelium hyperplasia and thickening of the alveolar septum were observed in the Model group. The immune phenomenon in the lung bronchus in the 0% GA group was weaker than that in the Model group. It could thus be inferred that PP sensitization decreased under the action of high temperature, high pressure and mechanical shear during extrusion. After the addition of GA, the alveolar interval and the degree of tissue damage was reduced in the mice, among which the lung tissue structure of mice in the 8% GA group was the most complete and clear. The results showed that the lung and intestinal tissue damage caused by PP allergy was minimal when 8% GA was added, and sensitization to PP could be reduced most effectively.

3.10 Analysis of the specific antibodies IgE, IgG1 and IgG2a

Food allergy symptoms are mainly caused by specific IgE that mediate the release of hypersensitive mediators from mast cells and basophils[53]. A specific antibody response is an indicator by which allergen sensitization can be directly evaluated, while serum immunoglobulin levels are the most commonly used indicators of the degree of a specific antibody response[54]. As shown in Figs. 12A-C, compared with the NS group, the serum-specific antibody content in the mice in the Model group was significantly increased ($P < 0.05$). The contents of IgE, IgG1 and IgG2a increased from 8.32 ng/mL to 10.52 ng/mL, 12.00 ng/mL to 16.57 ng/mL and 6.56 ng/mL to 8.69 ng/mL, respectively. The results were consistent with the

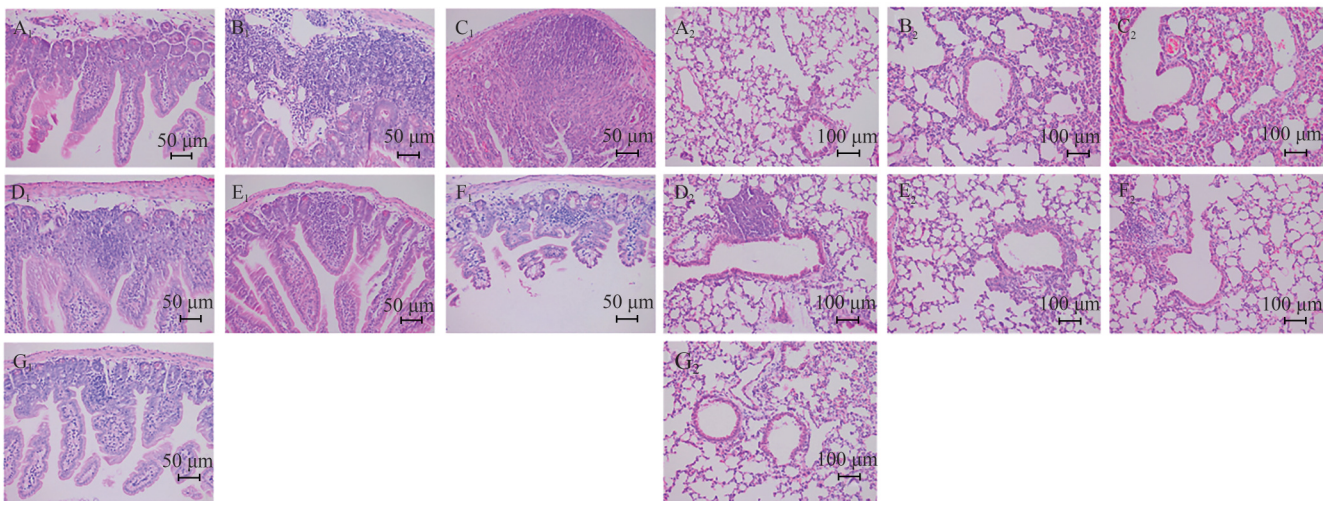

Fig. 11 Sections of the jejunum and lung were observed under an optical microscope. (A_1-G_1) Jejunum and (A_2-G_2) lung. (A) NS, (B) PP, (C) EPP, (D) EPP-2% GA, (E) EPP-4% GA, (F) EPP-6% GA, and (G) EPP-8% GA.

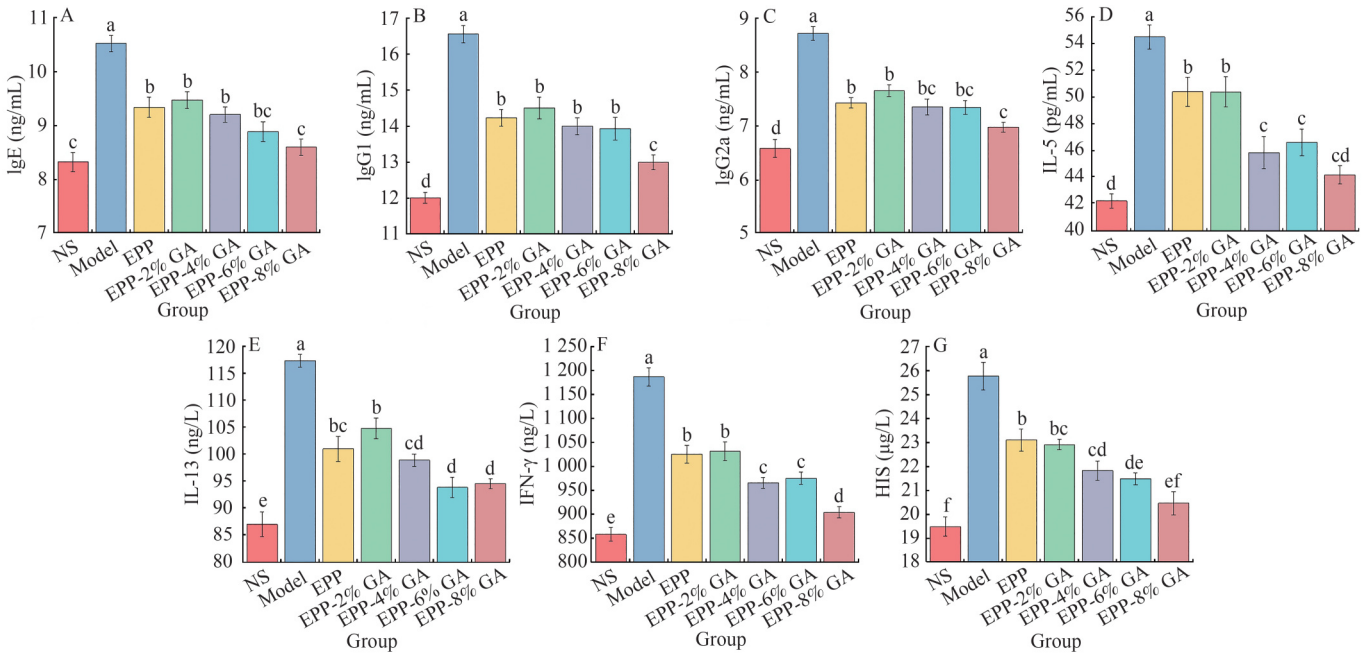

Fig. 12 Changes in the levels of specific antibodies (IgE, IgG1, and IgG2a), cytokines (IL-5, IL-13, and IFN-γ) and HIS in the serum of mice in each group. (A) IgE, (B) IgG1, (C) IgG2a, (D) IL-5, (E) IL-13, (F) IFN-γ, and (G) HIS.

research of Yu et al.[55], and the serum levels of specific antibodies IgE, IgG1 and IgG2a in BALB/c type mice were significantly increased after epidermal sensitization ($P < 0.01$). However, the serum-specific antibody content in the GA group was lower than that in the Model group. Except for the 8% GA group, there were no significant differences in the other GA groups ($P > 0.05$). Additionally, the serum specific antibody content in the 8% GA group was the lowest, and the contents of IgE, IgG1 and IgG2a were 8.59, 13.00 and 6.95 ng/mL, respectively. Therefore, sensitization in the EPP-8% GA group was the lowest. The ability of PP to bind specific antibodies is related to the linear epitope and conformational epitope of the protein. The decreased sensitization to the PP-GA complex may be due to the interaction between GA and PP, which directly covers the binding sites of some specific antibodies[56]. Moreover, the addition of GA led to changes in the secondary and tertiary structures of PP, and since the conformational epitopes are related to the structure of PP, this affected the binding of PP to specific antibodies, thereby reducing sensitization to PP.

3.11 IL-5, IL-13, IFN-γ, and HIS content analysis

IL-5, IL-13, and IFN-γ are Th2 cytokines that are involved in Th2 differentiation and IgE isomerization. IFN-γ is a Th1 cytokine that causes IgG2a isoconversion[57]. As shown in Figs. 12D-F, the contents of IL-5, IL-13 and IFN-γ in the serum of mice in the NS group were 42.28 pg/mL, 87.08 ng/L and 857.89 ng/L, respectively; additionally, the contents of cytokines in this group were very small, indicating that the immune response of the mice in the NS group was very weak. Compared with the NS group, the serum contents of IL-5, IL-13 and IFN-γ in the Model group were significantly increased ($P < 0.05$) to 54.43 pg/mL, 117.408 ng/L and 1 186.28 ng/L, respectively. This showed that PP stimulated a severe immune response in these mice and many related cytokines were secreted. The contents of serum cytokines (IL-5, IL-13, and IFN-γ) in the GA group were significantly lower than those in the Model group ($P < 0.05$). These results showed the following: 1) the extent of the immune response induced by PP after high water extrusion is relatively mild, that is, high water extrusion treatment could reduce PP sensitization to a certain extent, possibly because the IgE binding epitope of the sensitized protein was destroyed[58]; and 2) the combination of PP and GA can effectively inhibit the release of cytokines and reduce sensitization to PP. As the GA concentration increased from 0% to 8%, the serum cytokine content in mice showed a generally decreasing trend. When the GA supplementation was 8%, the contents of IL-5, IL-13 and IFN-γ were reduced by 18.81%, 19.43% and 23.82%, respectively, compared with those in the Model group.

HIS in serum is mainly produced by mast cells and basophil degranulation and can reflect the severity of an allergic reaction[59]. As shown in Fig. 12G, there was a significant difference in HIS content in serum between the NS group and Model group ($P < 0.05$), giving values of 19.47 and 25.75 μg/L, respectively. The HIS content in serum in the GA group was lower than that in the Model group, and as the GA content increased, the HIS content gradually decreased. When GA supplementation reached 8%, the HIS content in the serum of mice was 20.45 μg/L, and there was no significant difference between this group and the NS group ($P > 0.05$). The results showed that GA could inhibit the release of HIS in mice, and as more GA was added in the range of 0% – 8%, the stronger the inhibition was. Therefore, it can be inferred that PP combined GA could reduce sensitization to PP.

4. Conclusion

After BALB/c mice were intraperitoneally injected with the PP-GA complex with a GA concentration of 8%, the contents of serum specific antibodies (IgE, IgG1, and IgG2a) were 8.59 ng/mL, 13.00 ng/mL and 6.95 ng/mL, respectively. Additionally, the release of cytokines (IL-5, IL-13, and IFN-γ) and HIS decreased by 18.81%, 19.43% and 23.82%, respectively. Moreover, the average allergy

symptom score of these mice dropped to 1.71, and the aggregation of mast cells and basophils was significantly reduced. In addition, this group of mice also had the least damage to their spleen, intestinal and lung tissues. Sensitization to PP after treatment with EPP-8% GA was the lowest, which is due to the interaction between PP and GA under high moisture extrusion conditions, which increases the content of free sulfhydryl groups, decreases the number of disulfide bonds, and changes the PP secondary structure from random coils/β-turns to more α-helices/β-sheets. Our results indicate that high moisture extrusion of PP combined with GA is a feasible and effective method to reduce PP sensitization, which is of great significance when studying reducing PP sensitization with plant polyphenols.

Conflict of interest

All authors declare no conflict of interest.

Acknowledgements

This work was supported by the Natural Science Foundation of China (32072139) and Liaoning Province Natural Science Foundation Project (2022-MS-307).

References

[1] D. Seth, P. Poowutikul, M. Pansare, et al., Food allergy: a review, Pediatr. Ann. 49 (2020) 50-58. https://doi.org/10.3928/19382359-20191206-01.

[2] N. A. David, A. Penumarti, A. W. Burks, et al., Food allergen extracts to diagnose food-induced allergic diseases: how they are made, Ann. Allerg. Asthma. Im. 119 (2017) 101-107. https://doi.org/10.1016/j.anai.2016.11.008.

[3] R.L. Peters, M. Krawiec, J.J. Koplin, et al., Update on food allergy, Pediatr Allergy Immu. 32 (2021) 647-657. https://doi.org/10.1111/pai.13443.

[4] C. Kanagaratham, Y.S. El Ansari, O.L. Lewis, et al., IgE and IgG antibodies as regulators of mast cell and basophil functions in food allergy, Front. Immuno. 11 (2020) 603050. https://doi.org/10.3389/fimmu.2020.603050.

[5] J.J. Koplin, R.L. Peters, K.J. Allen, et al., Prevention of food allergies, Immunol. Allergy Clin. N. A.38 (2018) 1-11. https://doi.org/10.1016/j.iac.2017.09.001.

[6] T. Tian, K. Y. Ren, X. R. Cao, et al., High moisture extrusion of soybean-wheat co-precipitation protein: mechanism of fibrosis based on different extrusion energy regulation, Food Hydrocoll. 144 (2023) 108950. https://doi.org/10.1016/j.foodhyd.2023.108950.

[7] J.J. Yu, P.Y. Jiang, S.H. Li, et al., Mechanism of improving interfacial hydration characteristic of high-denatured peanut protein induced by cold plasma, J. Food Process Eng. 45 (2022) e13926. https://doi.org/10.1111/jfpe.13926.

[8] X.X. Han, Y.L. Zhao, S.N. Mao, et al., Effects of different amounts of corn silk polysaccharide on the structure and function of peanut protein isolate glycosylation products, Foods 11 (2022) 2214. https://doi.org/10.3390/foods11152214.

[9] A. Rana, M. Samtiya, T. Dhewa, et al., Health benefits of polyphenols: a concise review, J. Food Biochem. 46 (2022) e14264. https://doi.org/10.1111/jfbc.14264.

[10] C. Bessa, T. Francisco, R. Dias, et al., Use of polyphenols as modulators of food allergies. from chemistry to biological implications, Front. Sustain Food S. 5 (2021) 623611. https://doi.org/10.3389/fsufs.2021.623611.

[11] W.Y. He, T.T. Zhang, T.C. Velickovic, et al., Covalent conjugation with (−)-epigallo-catechin 3-gallate and chlorogenic acid changes allergenicity and functional properties of Arah1 from peanut, Food Chem. 331 (2022) 127355. https://doi.org/10.1016/j.foodchem.2020.127355.

[12] N.J. Plundrich, R.R. Bansode, E.A. Foegeding, et al., Protein bound vaccinium fruit polyphenols decrease IgE binding to peanut allergens and RBL-2H3 mast cell degranulation *in vitro*, Food Funct. 8 (2017) 1611-1621. https://doi.org/10.1039/c7fo00249a.

[13] R.C. Strauch, M.A. Lila, Pea protein isolate characteristics modulate functional properties of pea protein-cranberry polyphenol particles, Food Sci. Nutr. 9 (2021) 3740-3751. https://doi.org/10.1002/fsn3.2335.

[14] J.G. Li, M.M. Wu, Y. T. Wang, et al., Effect of pH-shifting treatment on structural and heat induced gel properties of peanut protein isolate, Food Chem. 325 (2020) 126921. https://doi.org/10.1016/j.foodchem.2020.126921.

[15] Y. Zhang, M. Song, J.Y. Xu, et al., IgE recognition and structural analysis of disulfide bond rearrangement and chemical modifications in allergen aggregations in roasted peanuts, J. Agri. Food Chem. 71 (2023) 9110-9119. https://doi.org/10.1021/acs.jafc.3c01482.

[16] M. Hayta, B. Benli, E.M. Iscimen, et al., Optimization of antihypertensive and antioxidant hydrolysate extraction from rice bran proteins using ultrasound assisted enzymatic hydrolysis, J. Food Meas. Charact. 14 (2020) 2578-2589. https://doi.org/10.1007/s11694-020-00504-2.

[17] Y.Y. Han, M. Yu, L.J, Wang, Preparation and characterization of antioxidant soy protein isolate films incorporating licorice residue extract, Food Hydrocoll. 75 (2018) 13-21. https://doi.org/10.1016/j.foodhyd.2017.09.020.

[18] J.C. Zhang, Q.L. Chen, L. Liu, et al., High-moisture extrusion process of transglutaminase-modified peanut protein: effect of transglutaminase on the mechanics of the process forming a fibrous structure, Food Hydrocoll. 112 (2021) 106346. https://doi.org/10.1016/j.foodhyd.2020.106346.

[19] C. Liu, C. Chen, X. Yan, et al., Assessment of immune responses and intestinal flora in BALB/c mice model of wheat food allergy via different sensitization methods, Food Sci. Hum. Well. 3 (2023) 871-881. https://doi.org/10.1016/j.fshw.2022.09.016.

[20] B.C. van Esch, S. Abbring, M.A. Diks, et al., Post-sensitization administration of non-digestible oligosaccharides and Bifidobacterium breve M-16V reduces allergic symptoms in mice, Immun. Inflamm. Dis. 4 (2016) 155-165. https://doi.org/10.1002/iid3.101.

[21] R.J. Qi, Study of the effects and mechanisms of active constituents from *Forsythiae Fructus* on immediate hypersensitivity reactions, PUMC. 2023. https://doi.org/10.27648/d.cnki.gzxhu.(2022).000285.

[22] Y. Dai, M.J. Huang, Y.J. Xu, et al., Enzymatic hydrolysis of silkworm pupa and its allergenicity evaluation by animal model with different immunization routes, Food Sci. Hum. Well. 12 (2022) 774-782 https://doi.org/10.1016/j.fshw.2022.09.011..

[23] S. Soares, M. S. Silva, I. García-Estévez, et al., Effect of malvidin-3-glucoside and epicatechin interaction on their ability to interact with salivary proline-rich proteins, Food Chem. 276 (2019) 33-42. https://doi. org/10.1016/j.foodchem.2018.09.167.

[24] H. Jin, L.Z Jiang, H.Y. Feng, et al., Effects of covalent and non-covalent interaction with chlorogenic acid on the stability and antioxidant activity of black soybean protein isolate-stabilized nanoemulsion, Food Sci. 43 (2022) 17-24. https://doi.org/1002-6630(2022)43:4<17:LYSGJH>2.0.TX;2-O.

[25] X.W. Pi, Y.X. Sun, G.M. Fu, et al., Effect of processing on soybean allergens and their allergenicity, Trends Food Sci. Tech. 118 (2021) 316-327. https://doi.org/10.1016/j.tifs.2021.10.006.

[26] H.B. Mi, Y. Li, C. Wang, et al., The interaction of starch-gums and their effect on gel properties and protein conformation of silver carp surimi, Food Hydrocoll. 112 (2021) 106290. https://doi.org/10.1016/j.foodhyd.2020.106290.

[27] F.L. Chen, Y.M. Wei, B. Zhang, Chemical cross-linking and molecular aggregation of soybean protein during extrusion cooking at low and high moisture content, LWT-Food Sci. Tcechnol. 44 (2011) 957-962. https://doi.org/10.1016/j.lwt.2010.12.008.

[28] F.G. Liu, C.X. Sun, W. Yang, et al., Structural characterization and functional evaluation of lactoferrin-polyphenol conjugates formed by free-radical graft copolymerization, RSC Advances. 5 (2015) 15641-15651. https://doi.org/10.1039/c4ra10802.

[29] X.N. Sui, H.N. Sun, B.K. Qi, et al., Functional and conformational changes to soy proteins accompanying anthocyanins: focus on covalent and non-covalent interactions, Food Chem. 245 (2018) 871-878. https://doi.org/10.1016/j.foodchem.2017.11.090.

[30] Y. Meng, C. Li, Conformational changes and functional properties of whey protein isolate-polyphenol complexes formed by non-covalent interaction, Food Chem. 364 (2021) 129622. https://doi.org/10.1016/j.foodchem.2021.129622.

[31] R.W. Visschers, H.H.J. de Jongh, Disulphide bond formation in food protein aggregation and gelation, Biotechnology Adv. 25 (2005) 75-80. https://doi.org/10.1016/j.biotechadv.2004.09.005.

[32] D. Apostolovic, J.T. Marsh, J. Baumert, et al., Purification and initial characterization of Arah 7, a peanut allergen from the 2S albumin protein

family, J. Agricultural. Food Chem. 69 (2021) 6318-6329. https://doi.org/10.1021/acs.jafc.1c00618.

[33] S. Filep, D.S. Block, B.R.E Smith, et al., Specific allergen profiles of peanut foods and diagnostic or therapeutic allergenic products, J. Allergy Clin. Immun. 141 (2018) 626-631. https://doi.org/10.1016/j.jaci.2017.05.049.

[34] Y.Q. Liu, Y.Y. Huang, X.Q. Deng, et al., Effect of enzymatic hydrolysis followed after extrusion pretreatment on the structure and emulsibility of soybean protein, Process Biochem. 116 (2022) 173-184. https://doi.org/10.1016/j.procbio.2022.03.012.

[35] X.S. Yu, H.G. Wang, Y. Yuan, et al., Changes in physicochemical and structural properties of pea protein during the high moisture extrusion process: effects of carboxymethylcellulose sodium and different extrusion zones, IJBM. 251 (2023) 12635. https://doi.org/10.1016/j.ijbiomac.2023.126350.

[36] D.Y. Yang, S. Gao, H.S. Yang, et al., Effects of sucrose addition on the rheology and structure of iota-carrageenan, Food Hydrocoll. 99 (2020) 105317. https://doi.org/10.1016/j.foodhyd.2019.105317.

[37] J. Wei, D.X. Xu, J. Yang, et al., Analysis of the interaction mechanism of Anthocyanins (*Aronia melanocarpa* Elliot) with beta-casein, Food Hydrocoll. 84 (2018) 276-281. https://doi.org/10.1016/j.foodhyd.2018.06.011.

[38] C. Li, L.X. Wang, F. Xue, et al., Effects of conjugation between proteins and polysaccharides on the physical properties of emulsion-based edible films, J. Am. Oil Chem. Soc. 96 (2019) 1249-1263. https://doi.org/10.1002/aocs.12278.

[39] Y.C. Liu, Z.Y. Yang, J. Du, et al., Interaction of curcumin with intravenous immunoglobulin: a fluorescence quenching and Fourier transformation infrared spectroscopy study, Immunobiology. 213 (2008) 651-661. https://doi.org/10.1016/j.imbio.2008.02.003.

[40] X.Y. Sun, W. Zhang, L.F. Zhang, et al., Molecular and emulsifying properties of arachin and conarachin of peanut protein isolate from ultrasound-assisted extraction, LWT-Food Sci. Technol. 132 (2020) 109790. https://doi.org/10.1016/j.lwt.2020.109790.

[41] P. Wang, K.X. Liu, R.Q. Yang, et al., Comparative study on the bread making quality of normoxia and hypoxia-germinated wheat: evolution of γ-aminobutyric acid, starch gelatinization, and gluten polymerization during steamed bread making, J. Agr. Food Chem. 6 (2019) 3480-3490. https://doi.org/10.1021/acs.jafc.9b00200.

[42] W.J. Zhang, P.P. Zhao, J.Z. Li, et al., Effects of ultrasound synergized with microwave on structureand functional properties of transglutaminase-crosslinked whey protein isolate, USC. 83 (2022) 105935. https://doi.org/10.1016/j.ultsonch.2022.105935.

[43] M. Carbonaro, P. Maselli, A. Nucara, Relationship between digestibility and secondary structure of raw and thermally treated legume proteins: a Fourier transform infrared (FT-IR) spectroscopic study, Amino Acids 43 (2012) 911-921. https://doi.org/10.1007/s00726-011-1151-4.

[44] S.M. Zhao, L.Z. Jiang, D.M. Wang, et al., Regulation mechanism of epigallocatechin gallate on the structure of soybean protein, Food Sci. 42 (2021) 67-75. https://doi.org/1002-6630(2021)42:12<67:EDDDDB>2.0.TX;2-J.

[45] A.S.R. Ballegaard, K.L. Bogh, Intestinal protein uptake and IgE-mediated food allergy, Food Res. Int. 163 (2022) 112150. https://doi.org/10.1016/j.foodres.2022.112150.

[46] C.W. Sang, Q. Bai, X.P. Feng, et al., Optimized extraction of cAMP from jujube by ultra-high pressure technology and the anti-allergic effect for peanut allergy mouse, Front. Nutr. 9 (2022) 862900. https://doi.org/10.3389/fnut.2022.862900.

[47] A. Alim, T. Li, T. Nisar, et al., Polyphenols and pectin enriched golden kiwifruit (*Actinidia chinensis*) alleviates high fructose-induced glucolipid disorders and hepatic oxidative damage in rats: in association with improvement of fatty acids metabolism, Food Sci. Hum. Well. 12 (2023) 1872-1884. https://doi.org/10.1016/j.fshw.2023.02.039.

[48] X. Xiao, O.L. Erukainure, M.S. Islam, et al., Red honeybush (*Cyclopia genistoides*) tea mitigates oxidative imbalance and hyperlipidemia, while improving glucose homeostasis in type 2 diabetic rats, Food Sci. Hum. Well. 12 (2023) 2029-2039. https://doi.org/10.1016/j.fshw.2023.03.018.

[49] J. Zeng, M.D. Song, T. Jia, et al., Immunomodulatory influences of sialylated lactuloses in mice, Biochem. Biophys. Res. Commun. 514 (2019) 351-357. https://doi.org/10.1016/j.bbrc.2019.04.157.

[50] Y.M. Zhou, H.Y. Lu, S. Zhao, et al., The beneficial effects of Tartary buckwheat (*Fagopyrum tataricum* Gaertn.) on diet-induced obesity in mice are related to the modulation of gut microbiota composition, Food Sci. Hum. Well. 12 (2023) 1323-1330. https://doi.org/10.1016/j.fshw.2022.10.014.

[51] P. Vadas, B.B. Perelman, G.G. Liss, Platelet activating factor, histamine and tryptase levels in human anaphylaxis, J. Allergy Clin. Immun. 131 (2012) 144-149. https://doi.org/10.1016/j.jaci.2007.12.1125.

[52] S.Y. Jung, H.J. See, D.A. Kwon, et al., Silkworm dropping extract regulates food allergy symptoms via inhibition of Th2-related responses in an ovalbumin-induced food allergy model, J. Sci. Food Agric. 99 (2019) 7008-7015. https://doi.org/10.1002/jsfa.9993.

[53] E.L. Choi, N. Taheri, E. Tan, et al., The crucial role of the interstitial cells of cajal in neurointestinal diseases, Biomolecules. 19 (2023) 9. https://doi.org/10.3390/biom13091358.

[54] L. Castan, K.L. Bogh, N.Z. Maryniak, et al., Overview of *in vivo* and *ex vivo* endpoints in murine food allergy models: suitable for evaluation of the sensitizing capacity of novel proteins? Allergy 75 (2020) 289-301. https://doi.org/10.1111/all.13943.

[55] G. Yu, Y. Jiang, S. Zhang, et al., Comparison of immune responses and intestinal flora in epicutaneously sensitized BALB/c or C57BL/6 mouse models of food allergy, Food Sci. Hum. Well. 13(2) (2024) 668-680. https://doi.org/10.26599/FSHW.2022.9250056.

[56] Q. Geng, Y. Zhang, M. Song, et al., Allergenicity of peanut allergens and its dependence on the structure, Compr. Rev. Food Sci. Food. 22 (2023) 1058-1081. https://doi.org/10.1111/1541-4337.13101.

[57] S. Kumar, Y. Jeong, M.U. Ashraf, et al., Dendritic cell-mediated Th2 immunity and immune disorders, Int. J. Mol. Sci. 20 (2019) 2159. https://doi.org/10.3390/ijms20092159.

[58] T.G. Pan, Y.N. Wu, S.D. He, et al., Food allergenic protein conjugation with plant polyphenols for allergenicity reduction, Curr. Opin. Food Sci. 43 (2022) 36-42. https://doi.org/10.1016/j.cofs.2021.10.002.

[59] S.E. Lavens, D. Proud, J.A. Warner, et al., A sensitive colorimetric assay for the release of tryptase from human lung mast cells *in vitro*, J. Immuno. Methods 166 (1993) 93-102. https://doi.org/10.1016/0022-1759(93)90332-2.